Hot electron transport in a strongly correlated transition-metal oxide

Rana, Kumari Gaurav; Yajima, Takeaki; Parui, Subir; Kemper, Alexander F.; Devereaux, Thomas P.; Hikita, Yasuyuki; Hwang, Harold Y.; Banerjee, Tamalika

Published in:
Scientific Reports

DOI:
10.1038/srep01274

Publication date:
2013

Supplementary Information: Hot electron transport in a strongly correlated transition metal oxide

Kumari Gaurav Rana[1], Takeaki Yajima[2,3], Subir Parui[1], Alexander F. Kemper[3], Thomas P. Devereaux[3], Yasuyuki Hikita[3], Harold Y. Hwang[3,4] and Tamalika Banerjee[1,*]

[1] *Physics of Nanodevices, Zernike Institute for Advanced Materials, University of Groningen, The Netherlands*

[2] *Department of Materials Engineering, The University of Tokyo, Bunkyo-ku, Tokyo, 113-8656, Japan*

[3] *Stanford Institute for Materials and Energy Sciences, SLAC National Accelerator Laboratory, Menlo Park, California 94025, USA and*

[4] *Geballe Laboratory for Advanced Materials, Department of Applied Physics, Stanford University, Stanford, California 94305, USA*

(Dated: January 27, 2013)

* T.Banerjee@rug.nl

Apart from BEEM measurements, LSMO/Nb:STO Schottky junctions were characterized by three different techniques. In current-voltage (I-V) measurements (Fig. S1a), all the junctions showed a clear rectification behavior with a linear relationship between log I and V in the forward bias region (V is applied to the LSMO films). The ideality factor calculated from the slope of this linear region was close to unity, indicating that the current is dominated by thermionic emission[1]. The linear region was extrapolated, and the current intercept (I_0) gives ϕ_B via the formula, $\frac{kT}{e}\left(ln\left[AT^2\right] - lnI_0\right)$, where k is the Boltzmann constant, T is the measurement temperature, e is the elementary charge, and A is the Richardson constant[1]. In capacitance-voltage (C-V) measurements (Fig. S1b), $1/C^2$ was a linear function of V for all the LSMO thicknesses in accordance with the Mott-Schottky model[1]. The voltage intercept of the linear extrapolation corresponds to the built-in potential (V_{bi}) in the semiconductor, which is related to ϕ_B via ϕ_B-$V_{bi} \sim 0.1$ eV. Here the gap between the ϕ_B and V_{bi} was estimated using the electronic effective mass of 1.5 m_0 , 1.5 m_0, and 15 m_0 in three crystallographic directions of STO[2, 3], where m_0 denotes the free electron mass. The slope of this linear function, reflecting the dopant concentration and the permittivity of the semiconductor in general, has some sample-to-sample variations due to slightly different Nb concentrations at this low density (the nominal value is 0.01 wt. %). Internal photoemission (IPE) spectroscopy was performed (Fig. S1c) to show a linear relationship between the square root of photoyield (photocurrent per photon) and the photon energy[4]. The linear region was extrapolated and the intercept of the photon energy equals to the ϕ_B. In Fig. S1d, the ϕ_B values from each measurement are plotted as a function of the LSMO film thickness, showing the values $1.0 \sim 1.1$ eV with only a small fluctuation for different LSMO thicknesses or measurement techniques.

The attenuation length is modeled based on the available phase space for scattering, as discussed in Zarate *et al* [5]. We constructed a model for the electronic density of states (DOS) based on the Density Functional Theory (DFT) results from Pickett and Singh [6]. The model consisted of a featureless DOS (for the majority spin) at the Fermi level, combined with a larger DOS at 1.8 eV below the Fermi level for the majority spin, and a linear DOS starting at the Fermi level for the minority spin. The band velocity was estimated by a

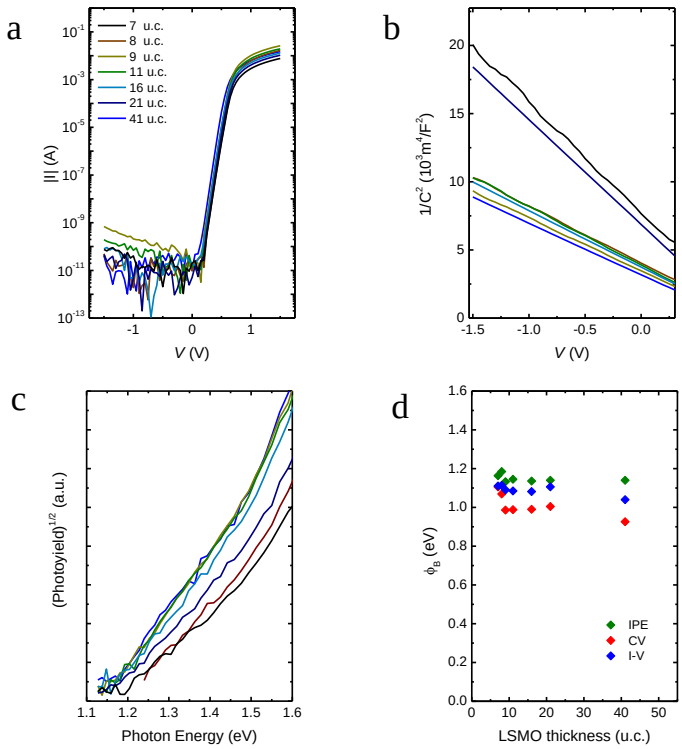

FIG. S1. **Schottky junction properties.** a. I-V characteristics, b. C-V characteristics and c. IPE spectra for LSMO/Nb:STO heterostructures with varied LSMO film thicknesses. d. ϕ_B from the various measurements are summarized.

simple cosine model. As described in the main text, the electron-electron scattering rate was combined through Matthiessen's rule with a polaronic scattering rate. At relatively high injection energies, the polaronic scattering rate is assumed to be energy-independent. Using the overall scale for the velocity, the electron-electron scattering matrix element, and the mean free path due to the polaronic scattering as fitting parameters, we arrive at the curve shown in Fig. 3 (main text).

It is interesting to note that electron-phonon scattering within the Migdal limit is not sufficiently strong to arrive at the experimentally observed attenuation length. For reasonable values of the electron-phonon coupling constant λ, the attenuation length based on an empirical model of electron-phonon scattering is many times longer than the observed energy-independent attenuation length.

The extracted hot electron attenuation length for different transition metal ferromagnets

Metals	λ_{hot}	Energy	Ref.
Co (300 K)	2.1 nm	-1.5 V	7
Fe (150 K)	1.6 nm	-1.4 V	8
Ni (300 K)	3.2 nm	-1.4 V	9
Au (300 K)	26.5 nm	-1.2 V	10
Ag (80 K)	25 nm	-1.2 V	11
Cu (100 K)	30 nm	-1.1 V	12

TABLE I. List of values of hot electron attenuation lengths in transition metal ferromagnets and noble metals on Si (100) using Ballistic electron emission microscopy.

and noble metals on Si (100), obtained from Ballistic Electron Emission Microscopy studies, at different temperatures, are shown in Table 1.

[1] Sze, S. M. & Ng, K. K. "Physics of semiconductor devices", 3rd edn. (John Wiley & Sons, Hoboken, New Jersey 2007).

[2] Takizawa, M. *et al. Phys. Rev. B* **79,** 113103 (2009).

[3] Santander-Syro, A. F. *et al. Nature* **469,** 189-194 (2011).

[4] Fowler, R. H. *Phys. Rev.* **38,** 45-56 (1931).

[5] Zarate, E., Apell, P., & Echenique, P. M. *Phys. Rev. B* **60,** 2326-2332 (1999).

[6] Pickett, W. E., & Singh, D. J. *Phys. Rev. B* **53,** 1146-1160 (1996).

[7] Rippard, W. H., & Buhrman, R. A., *Phys. Rev. Lett.* **84**, 971 (2000).

[8] Banerjee, T., Lodder, J. C., & Jansen, R. *Phys. Rev. B* **76**, 140407 (2007).

[9] Parui, S., Rana, K. G., Bignardi, L., Rudolf, P., van Wees, B. J., & Banerjee, T. *Phys. Rev. B* **85**, 235416 (2012).

[10] Weilmeier, M. K., Rippard, W. H., & Buhrman, R. A. *Phys. Rev. B* **59**, R2521 (1999).

[11] Garramone, J. J., Abel, J. R., Barraza-Lopez, S., & LaBella, V. P. *Appl. Phys. Lett.* **100**, 252102 (2012).

[12] Parui, S., van der Ploeg, J. R. R., Rana, K. G., & Banerjee, T. *Phys. Status Solidi RRL* **5**, 388 (2011).